Chinese Journal of Physics 91 (2024) 220–236

Contents lists available at ScienceDirect

Chinese Journal of Physics

journal homepage: www.sciencedirect.com/journal/chinese-journal-of-physics

Research Paper

# Gaussian bistable cascade double feedback stochastic resonance weak signal enhancement detection

Shangbin Jiao [a,*], Tiantian Hou [a], Tingyang Jiao [b], Yi Wang [a], Nianlong Song [a]

[a] Shaanxi Key Laboratory of Complex System Control and Intelligent Information Processing, Xi'an University of Technology, Xi'an 710048, China
[b] Department of Information and Computing Sciences, Utrecht University, 3508 TC Utrecht, The Netherlands

ARTICLE INFO

*Keywords:*
Double feedback SR
Weak signal detection
Multi-system collaborative
Bearing fault detection

ABSTRACT

Stochastic resonance (SR), as a nonlinear weak signal enhancement detection method, has found extensive applications in fields like fault diagnosis and biological information processing. However, further research has revealed that single stochastic resonance systems often fail to meet the requirements of practical engineering applications, leading to a growing interest in multi-system collaborative stochastic resonance. This article first constructs a cascaded SR system based on the Gaussian bistable model, and introduces the idea of feedback into the cascaded system. A Gaussian bistable cascaded dual feedback SR system is proposed to improve the output signal enhancement performance of the system. This system effectively utilizes the memory characteristics inherent in the output feedback and enables multi-level particle transitions and energy transfers in noisy input signals, thereby reducing noise and enhancing the extraction of weak signal features. Furthermore, the BSO optimization algorithm was utilized to optimize the system parameters of the model, resulting in an adaptive Gaussian bistable cascaded double feedback stochastic resonance (GBCDFSR) system. This system is applied to the processing of noisy periodic signals across various noise types. Simulation experiments and engineering applications show that the proposed model has stronger signal detection capabilities.

## 1. Introduction

Stochastic resonance (SR) [1] theory represents a novel approach leveraging nonlinear dynamics and statistical physics to enhance the detection of weak signals . This method employs a nonlinear system that, under the influence of noisy signals, toggles the potential function between different states. This modulation transforms the noisy original signal into a high-amplitude transition signal that aligns with the frequency of the useful signal [2–5]. Some noise energy is converted into the signal energy to highlight the frequency characteristics of the signal and achieve enhanced detection of weak signals. Compared to traditional weak signal detection methods, SR utilizes noise rather than suppressing it, and can detect and extract features of weak signals under extremely low signal-to-noise ratio (SNR) conditions. This provides a new approach for weak signal detection and processing in strong noise backgrounds [6–10].

In nonlinear systems based on the SR model, the system's structure directly influences the crossing time and transition difficulty of Brownian particles between potential wells. This, in turn, affects the degree of noise energy transfer to the signal, ultimately impacting the detection performance of the nonlinear system for weak signals. Traditional SR systems often encounter output saturation and high potential barriers. However, the continuity and adjustability advantages of Gaussian models can alleviate some of these issues. Zhang

* Corresponding author.
*E-mail address:* jiaoshangbin@xaut.edu.cn (S. Jiao).

https://doi.org/10.1016/j.cjph.2024.07.026
Received 5 June 2024; Received in revised form 16 July 2024; Accepted 17 July 2024
Available online 19 July 2024
0577-9073/© 2024 The Physical Society of the Republic of China (Taiwan). Published by Elsevier B.V. All rights are reserved, including those for text and data mining, AI training, and similar technologies.

[9] and Jiao [10] combined the Gaussian potential model with traditional SR systems, demonstrating its superior performance. Li et al. proposed a new segmented nonlinear stochastic resonance (PNSR) system. The potential function of PNSR can be fine-tuned using a single parameter, effectively addressing both the output saturation and local optimization challenges in parameter optimization [11].

Apart from piecewise potential function models, some unsaturated continuous function models have also been extensively researched [12]. Cheng et al. introduced an adaptive smooth unsaturated bistable stochastic resonance (ASUBSR) system by integrating the Wood Saxon potential function and Gaussian function.

Recent research indicates that the multi-system cooperative SR system has increasingly gained the attention of scholars [13–14]. At present, common cooperative SR include parallel [15] SR, cascade SR and coupled [16,17] SR. The parallel SR system does not emphasize a single SR system, but highlights the collective effect of the whole system, which improves the output signal-to-noise ratio of the system to a certain extent and enhances the fault tolerance of a single system. However, the interaction between transverse subsystems is not considered in the parallel SR system. Although the coupling SR system enhances the synergy between the systems by introducing the coupling coefficient, enhances the connection between the systems to a certain extent, and improves the output of the system, it is the same as the parallel SR system, ignoring the repetitive processing ability of the longitudinal multi-level subsystem to the input signal, and there is still room for further improvement to a certain extent. In the cascaded SR system, the output of the previous system is used as the input of the next system, and the noise is further weakened by repeated processing of the input signal in the multi-level system, so as to realize the enhanced extraction of weak signal features [18]. However, with the increase of the number of cascade systems, the low-frequency signal in the system output signal is repeatedly enhanced, and the enhancement effect of the characteristic frequency is often not very ideal.

In response to the above issues, this paper proposes a Gaussian Bistable Cascaded Double Feedback (GBCDF) SR system, aimed at improving the SR method's ability to enhance and extract feature signals. The difference between this system and traditional SR systems is that it improves the utilization of noise energy through cascading, while utilizing output feedback to endow the system with corresponding memory characteristics. It not only enhances the target feature frequency, but also effectively suppresses signal components below that frequency, which can effectively enhance the extraction of fault feature frequency, significantly improve the signal-to-noise ratio of the output signal and the recognition of feature frequency.

## 2. System model

### *2.2.1. Classic bistable SR model*

The basic principle of SR is based on the Langevin equation:

$$\frac{dx}{dt} = -U(x) + s(t) + \sqrt{2D}\eta(t). \tag{1}$$

In the formula, $U(x)$ is the potential function, D is the noise intensity, $\eta(t)$ is the noise, represents the random disturbance force; $s(t)$ is the input signal, representing the excitation force. In the study of SR, nonlinear bistable models are widely used, namely:

$$U(x) = -\frac{a}{2}x^2 + \frac{b}{4}x^4. \tag{2}$$

This equation describes the over damped motion of a Brownian particle, which alternates back and forth between two potential

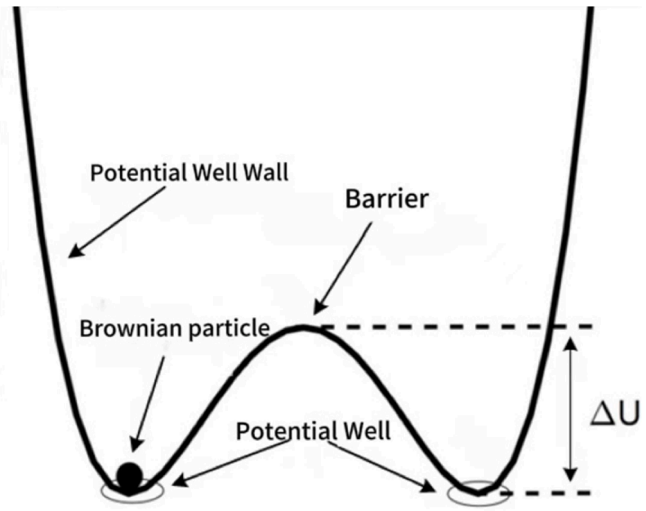


**Fig. 1.** Potential function of bistable system.

well points under the combined action of weak signals and noise. When there is no external signal input, taking the parameters $a = 1$ and $b = 1$ of the SR system, the potential function of the bistable SR system is obtained as shown in Fig. 1.

Brownian particles undergo periodic transitions in bistable systems. In the absence of noise, when the input signal amplitude $A$ is small and below the threshold $A_c\left(A_c = \sqrt{4a^3/27b}\right)$, particles cannot cross the middle potential barrier and oscillate in a single-sided potential well [19]; When $A$ is greater than the threshold, the particle undergoes a transition across the intermediate potential barrier due to the driving force. If the signal amplitude $A$ is too small, it is not possible to cross the intermediate barrier, and noise intervenes to achieve resonance, Brownian particles can successfully transition with the help of noise energy . When the output signal frequency of the SR system matches the input periodic signal frequency, signal enhancement can be achieved.

### 2.2.2. Gaussian SR model

The Gaussian model was first applied to nuclear physics, as it can accurately describe complex scattering phenomena and effectively derive feasible solutions to differential equations. Therefore, scholars have attempted to introduce the Gaussian model into SR to solve some model defect problems [20]. The Gaussian model can usually be represented by equation (3):

$$U = -V\exp\left(-\frac{x^2}{R^2}\right). \tag{3}$$

The Gaussian model achieves variation by adjusting parameters $V$ and $R$, presenting a single potential well structure. In Fig. (2) (a), with $R = 0.5$, the potential well depth of the Gaussian model increases with the increase of model parameter $V$; In Fig. (2) (b), let $V = 2$, gradually increase the value of $R$, and the potential well width of the Gaussian model also increases. The depth and width of the potential well in the Gaussian model are determined by the following values of $V$ and $R$, respectively, and there is no coupling effect between the two. Therefore, each parameter can be adjusted separately without affecting the other parameter, thereby fine-tuning the performance of the model.

### 2.2.3. Gaussian bistable cascaded double feedback stochastic resonance

This study is based on the feedback control concept in control theory, and introduces the feedback concept into cascaded systems to improve system performance and enhance the system output SNR. In a cascaded SR system, cascading enhances the system's full utilization of noise energy, while utilizing output feedback to give the system corresponding memory characteristics. Finally, it is proposed that the system exhibits the characteristics of a bandpass filter, which enhances the feature frequency while also effectively suppressing the signal components below the feature frequency. This significantly boosts the extraction of fault feature frequencies, substantially enhancing both the SNR of the output signal and the recognition of feature frequencies. Thus, to augment the extraction of weak signal features, GBCDFSR system is constructed, described as follows:

$$\begin{cases} \dfrac{dx_1(t)}{dt} = -\dfrac{\partial U_1(x_1)}{\partial x_1} + s(t) + \sqrt{2D}\eta(t) + k_1 x(t), \\ \dfrac{dx(t)}{dt} = -\dfrac{\partial U_2(x)}{\partial x} + x_1(t) + k_2 x(t). \end{cases} \tag{4}$$

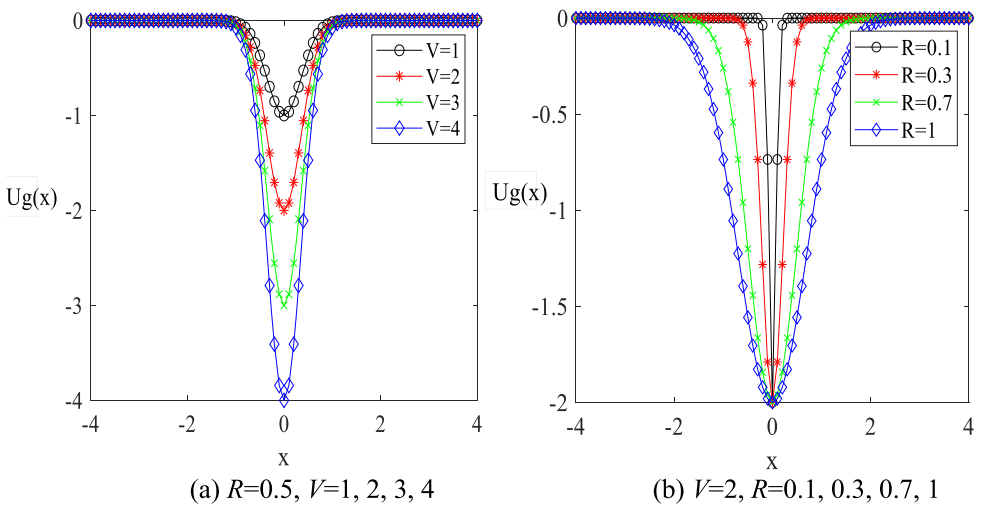


(a) $R$=0.5, $V$=1, 2, 3, 4 (b) $V$=2, $R$=0.1, 0.3, 0.7, 1

**Fig. 2.** Trend of gaussian model with parameter changes.

In the formula, $U_1(x_1) = \frac{a}{2}{x_1}^2 - \frac{b}{4}{x_1}^4, U_2(x) = -V\exp\left(-\frac{x^2}{R^2}\right), D$ is the noise intensity, $\eta(t)$is the noise, $s(t)$ is the input signal, and $k_1, k_2$ are the feedback coefficients. $x$ is the final output of the second level subsystem and cascading system, By introducing feedback parameters $k_1, k_2$ the output is respectively fed back to the first level subsystem and the second level subsystem to improve the dynamic response performance of the cascaded system.Fig. 3

To analyze the dynamic response performance of the proposed system, a fourth-order Runge Kutta numerical solution method was used to numerically solve the system output. Meanwhile, the introduction of scale transformation coefficients enables*l* the proposed system to be applied in large parameter signal processing in practical engineering.

$$\begin{cases} K_{11} = hl\big(-a(x_1[n]) + b(x_1[n])^3 + u[n] + k_1x[n]\big), \\ K_{12} = hl\big(-a(x_1[n] + K_{11}/2) + b(x_1[n] + K_{11}/2)^3 + u[n] + k_1x[n]\big), \\ K_{13} = hl\big(-a(x_1[n] + K_{12}/2) + b(x_1[n] + K_{12}/2)^3 + u[n+1] + k_1x[n]\big), \\ K_{12} = hl\big(-a(x_1[n] + K_{13}) + b(x_1[n] + K_{13})^3 + u[n+1] + k_1x[n]\big), \\ K_{21} = hl\big(-2VR(x[n])\exp\big(-\frac{x[n]^2}{R^2}\big) + u[n] + k_2x[n]\big), \\ K_{22} = hl\big(\big(-2VR(x[n])\exp\big(-\frac{x[n]^2}{R^2}\big) + K_{21}/2\big) + x_1[n] + k_2x[n]\big), \\ K_{23} = hl\big(\big(-2VR(x[n])\exp\big(-\frac{x[n]^2}{R^2}\big) + K_{22}/2\big) + x_1[n] + k_2x[n]\big), \\ K_{24} = hl\big(\big(-2VR(x[n])\exp\big(-\frac{x[n]^2}{R^2}\big) + K_{23}\big) + x_1[n] + k_2x[n]\big), \\ x_1[n+1] = x_1[n] + (K_{11} + 2K_{12} + 2K_{13} + K_{14})/6, \\ x[n+1] = x[n] + (K_{21} + 2K_{22} + 2K_{23} + K_{24})/6. \end{cases} \tag{5}$$

In the equation, $x(n)$ represents the nth discrete data of the output sequence of the nonlinear system, while the meanings of other parameters remain unchanged.

### 2.2.4. *System noise reduction evaluation indicators*

SR is a nonlinear phenomenon, and whether a system experiences SR requires some indicators to measure [21,22]. This article takes the output SNR, signal-to-noise ratio gain (SNRI), and average output SNR of the signal as evaluation indicators. The expression for SNR is:

$$SNR = \lim_{\Delta\omega\to 0}\int_{\omega-\Delta\omega}^{\omega+\Delta\omega} S(\omega)d\omega / S_N(\omega). \tag{6}$$

In equation (6): $S(\omega)$ is the signal power spectral density; $S_N(\omega)$ is the intensity of noise near the signal frequency. However, in the study of SR, scholars are more concerned about the enhancement and improvement effect of signal SR systems on input signals. Thus, the SNRI is introduced to assess the SR effect. Its expression is as follows:

$$SNR_{in} = 10\lg\left[SP(\omega)_{in} \,/\, NP(\omega)_{in}\right], \tag{7}$$

$$SNR_{\text{out}} = 10\lg\left[SP(\omega)_{\text{out}} \,/\, NP(\omega)_{\text{out}}\right], \tag{8}$$

hence, we have:

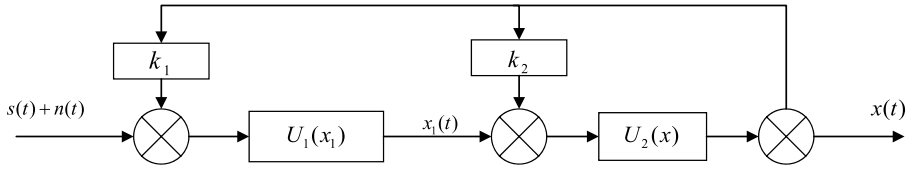


**Fig. 3.** Schematic diagram of the structure of GBCDFSR system.

$$SNRI = \frac{SP(\omega)_{\text{out}}/NP(\omega)_{\text{out}}}{SP(\omega)_{\text{in}}/NP(\omega)_{\text{in}}}. \tag{9}$$

Equations (7) and (8) respectively represent the system input and output SNR formulas, where $SP(\omega)_{\text{in}}$ and $SP(\omega)_{\text{out}}$ represent the signal power before and after random resonance, and $NP(\omega)_{\text{in}}$ and $NP(\omega)_{\text{out}}$ represent the average noise power of the system input and output at the input signal frequency. Equation (9) represents the SNRI. When SNRI is greater than 1, it indicates that the SR system has an enhancing and improving effect on the signal, and the larger the SNRI, the better the detection effect.

Using the average SNRI to quantify the detection performance of SR systems for multi frequency weak signals. Its expression is as follows:

$$MSNRI = \frac{1}{k}\sum_{i=1}^{k} SNRIi \; i = 1, 2, \cdots, k. \tag{10}$$

In Fig. 4, the parameters of the GBCDFSR model are set to$a = 9.5, b = 0.2, V = 0.8, R = 0.5, k_1 = -2, k_2 = -0.026$. The corresponding parameters of the bistable cascade system and the GBCDFSR system are processed by inputting the same signal $s(t) = A\sin(2\pi ft)$ under the same Gaussian noise background, where $A = 0.1, f = 0.01Hz$. By using the power spectrum method to calculate SNRI, it can be seen from the SNRI trend in Fig. 4 that in this state, the SNRI of the Gaussian bistable cascaded dual feedback SR system is higher than that of the bistable stage connected system, indicating that the GBCDFSR model has strong weak signal tracking ability.

## 3. System parameter impact

$\alpha$ noise is widely used in engineering and has a significant impact on wireless communication systems, radars, and other RF electronic devices. In engineering practice, dealing with noise is one of the important considerations for designing and maintaining these systems. Various technologies and methods are usually adopted to reduce or suppress noise to ensure that device performance and communication quality are not affected. Noise management is considered an important task in engineering as it directly affects the reliability and performance of modern communication and radar systems. Therefore, this section investigates the SR effect driven by signals under stable noise.

### 3.1. The variation law of MSNRI with system parameters under different $\alpha$ effects

Noise can capture more noise characteristics with different distributions. An example is selected as a signal $s(t) = A_1\sin(2\pi f_1 t) + A_2\sin(2\pi f_2 t) + A_3\sin(2\pi f_3 t)$ with $\alpha$ noise intensity D=0.1, where $A_1 = A_2 = A_3 = 0.01$ dynamically changes one parameter at a time while determining a set of parameter combinations. Using the power spectrum method, plot the average output signal-to-noise ratio gain (MSNRI) of the system as a function of the parameters. The curves shown in the article were all plotted using the average of 20 experiments. The specific experimental curve is shown in the following Fig. 5:

Firstly, fix a = 10.00, b = 0.75, V = 5.01, R = 3.66, k1 = −0.98, k2 = −0.03 so that the feature indices $\alpha$ are 0.5, 0.8, 1, 1.2, and 1.5 respectively, while keeping the other noise distribution parameters $\beta = 0, \sigma = 1, \mu = 0$ and input signal $s(t)$ unchanged. The variation curve of MSNRI with parameters obtained through simulation is shown in Fig. 5.

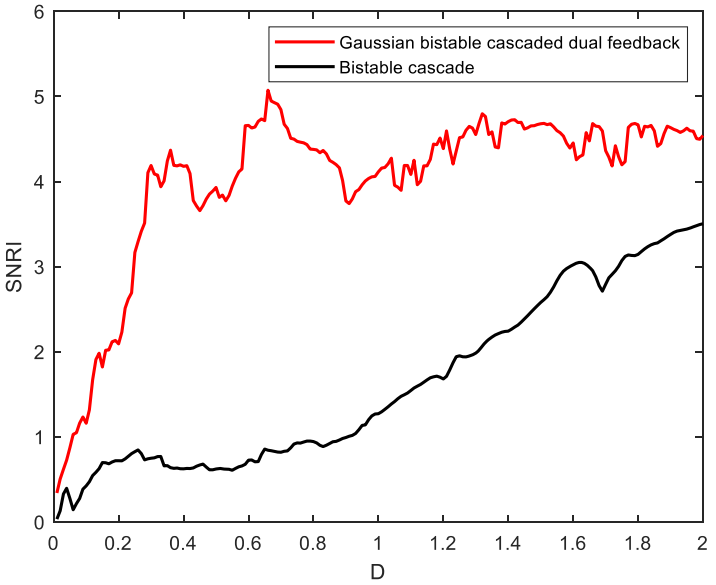


**Fig. 4.** Output SNR of different systems as a function of noise intensity.

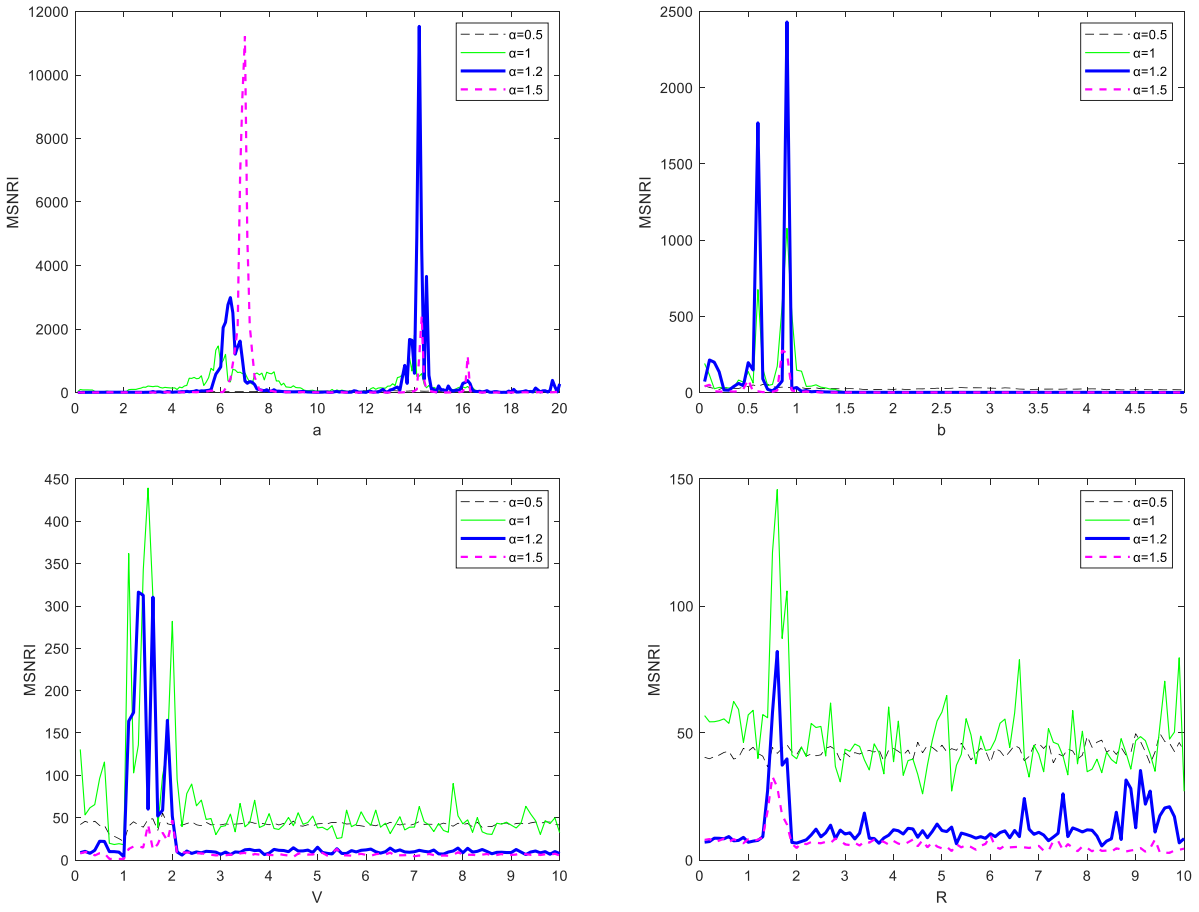


**Fig. 5.** Trend of output MSNRI with system parameters under different $\alpha$ effects.

As shown in Fig. 5, MSNRI exhibits multiple peaks with the variation of parameters, indicating that there are multiple intervals in which MSNRI can achieve random resonance with the variation of parameters. Particles surmount potential barriers and undergo periodic transitions between potential wells, leading to the phenomenon of SR, due to the combined influence of noise and the system.

Under this set of parameters, MSNRI exhibits multiple peaks with the variation of parameter a, increasing first and then decreasing in the intervals [5.86, 7.93] and [13.82–14.52], indicating that particles have crossed the potential barrier under the combined effect of noise and system, and are able to make periodic transitions between potential wells, resulting in SR phenomenon.

Similarly, when b is in the range of [0.52, 0.75], [0.75, 1.12], the matching degree between the input signal, noise, and the multi stable system gradually improves. When b is greater than 1.2, due to the insufficient energy required for the particle signal to cross the potential barrier, MSNRI gradually decreases until it reaches 0.

MSNRI exhibits multiple peaks with the variation of parameter V. In the interval [1.12, 2.13], the matching degree between the input signal, noise, and the multi stable system gradually improves. That is, when $V = 1.53$, MSNRI reaches its maximum value within this range, with the best matching degree and the best random resonance effect of the system. When V is greater than 2, due to insufficient energy required for the particle signal to cross the potential barrier, MSNRI gradually decreases.

When R increases from 1.22 – 1.98, the matching degree between the input signal, noise, and the multi stable system gradually improves. That is, when $R = 1.55$, the MSNRI reaches the maximum value within this range, with the best matching degree and the best system random resonance effect. When R is greater than 2, the MSNRI gradually decreases due to the insufficient energy required for the particle signal to cross the potential barrier.

Based on the aforementioned analysis, the following conclusions can be drawn: adjusting the system parameters can induce SR in the system, Realize GBCDFSR detection with multiple low-frequency weak signal excitations in a $\alpha$ stable noise environment.

### 3.2. *The variation law of MSNRI with system parameters under different $\beta$ effects*

Fix thea $= 10.00, \mathrm{b} = 0.75, \mathrm{V} = 5.01, \mathrm{R} = 3.66, \mathrm{k1} = -0.98, \mathrm{k2} = -0.03$,set the symmetric parameters $\beta$ to -1, 0, 1, and the remaining distribution parameters to$\alpha = 1.2, \sigma = 1, \mu = 0$. Keep the input signals$(t)$ unchanged. The simulation results show the variation curve of MSNRI with the parameters as shown in Fig. 6.

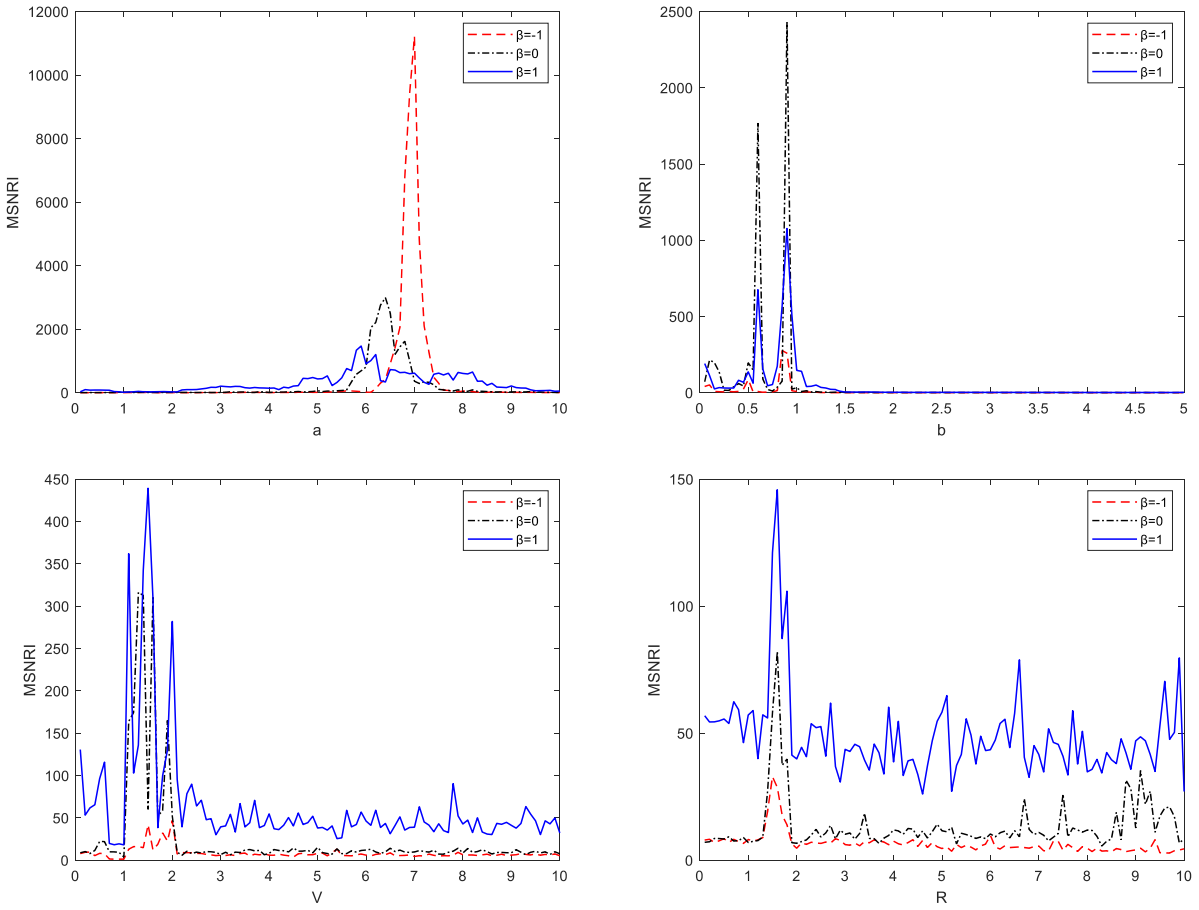


**Fig. 6.** Trend of output MSNRI with system parameters under different $\beta$ effects.

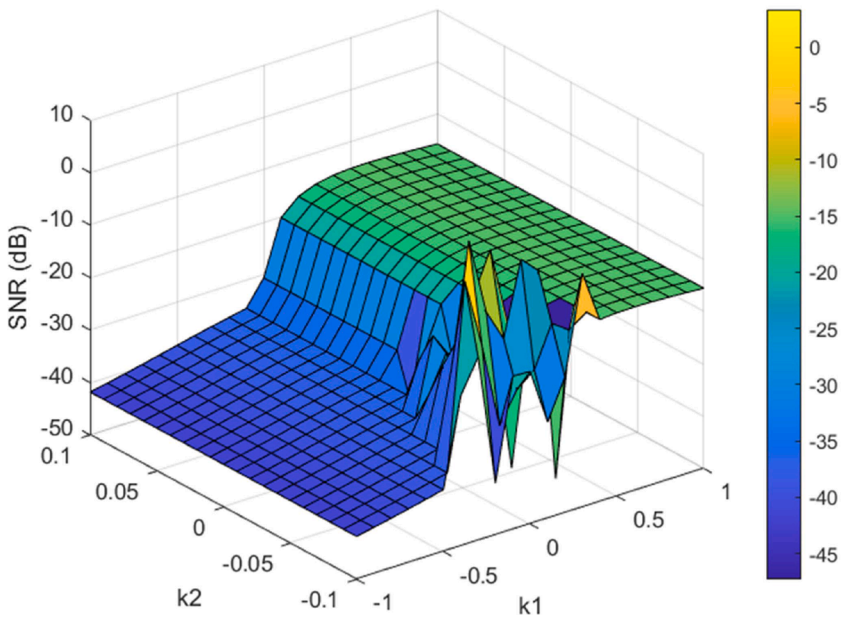


**Fig. 7.** Changes in SNR with k1 and k2 under $\alpha$ noise.

From Fig. 6, it can be seen that under the action of different symmetric parameters $\beta$, MSNRI exhibits multiple peaks as the parameters gradually increase. That is, MSNRI has multiple intervals that can achieve random resonance with the changes of parameters, all of which show a trend of first increasing and then decreasing. When the MSNRI reaches its maximum value with the curve waveform of the system parameters in different intervals, the input signal, noise, and the matching degree of the system are optimal.

From the above analysis, it can be seen that under the influence of different feature indices $\alpha$ or symmetric parameters $\beta$, studying the SR detection of multiple low-frequency weak signal excitations in a $\alpha$ stable noise environment, the average MSNRI has multiple intervals with the variation of parameters, which can achieve SR.

### 3.3. The influence of feedback coefficient on the SNR of SR output

This article is grounded in the concept of feedback control in control theory, introduces feedback technology into cascaded monostable systems to enhance system performance and boost the system's output SNR. In a cascaded SR system, the output from one system serves as the input for the subsequent system. By processing input signals repeatedly within multi-level systems, noise is further mitigated, leading to the enhanced extraction of weak signal features. Therefore, feedback coefficients $k_1$ and $k_2$ are introduced. We observe the effect of the introduced feedback coefficient on the output SNR with the same system input and parameter combination as in the previous text. The specific experimental curve is depicted in the figure below:

As shown in Figs. 7 and 8, when $k_2 > 0$, that is, when the second feedback is positive, only changing $k_2$ has a consistent impact on the output effect of the system, and cannot improve the output effect of the system. That is, the system cannot generate the optimal SR effect. When$k_2 < 0$, that is, when the second feedback is negative, $k_2$ exerts a more significant impact on the output of the SR system. Moreover, when $k_1 \in [0.2,0.6]$, the output SNR increases first and then decreases. When $k_1 = 0.3$, the SR effect of the system is the best.

As shown in Figs. 7 and 9, when $k_1 > 0.5$ and $k_1 < -0.5$, the change feedback coefficient $k_1$ has no significant impact on the output effect of the system and cannot improve its output effect. This indicates that in these cases, the system is not sensitive to changes in parameter $k_1$ and cannot achieve SR effects. When $-0.5 < k_1 < 0.5$,$k_1$ has a significant impact on the output of the SR system, and when $k_2 \in$ [-0.1, -0.04], the output SNR first increases and then decreases. Moreover, when $k_1 = -0.08$, the SR effect of the system is the best.

From this, it can be seen that the feedback coefficients $k_1$ and $k_2$ introduced in this article can significantly affect the output effect of the SR system. The optimal value range for $k_1 \in$[-0.5,0.5], and the optimal value range for $k_2 \in$ [-0.1,0]. Selecting appropriate parameter values within a specific range can enable the system to achieve the optimal state of SR effect.

### 3.4. Adaptive composite multisteady state stochastic resonance method

The output of a SR system is greatly influenced by system parameters, and its essence is global optimization. Particle Swarm Optimization (PSO) [23] and Brainstorming (BSO) [24] are the two most common global optimization algorithms, both of which search for the optimal solution through iteration. However, there are significant differences in their search strategies, optimization

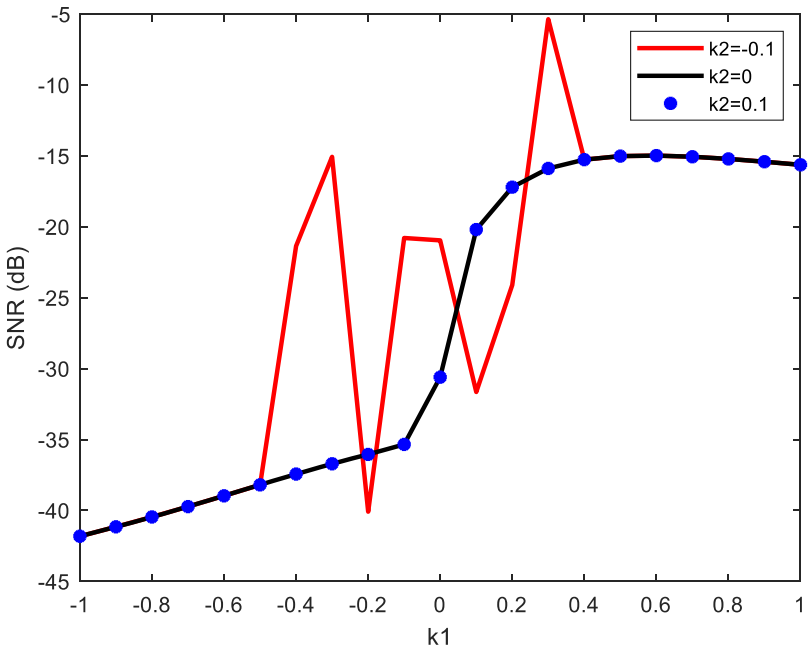


**Fig. 8.** Changes in SNR with k1 under different k2 effects of $\alpha$ noise.

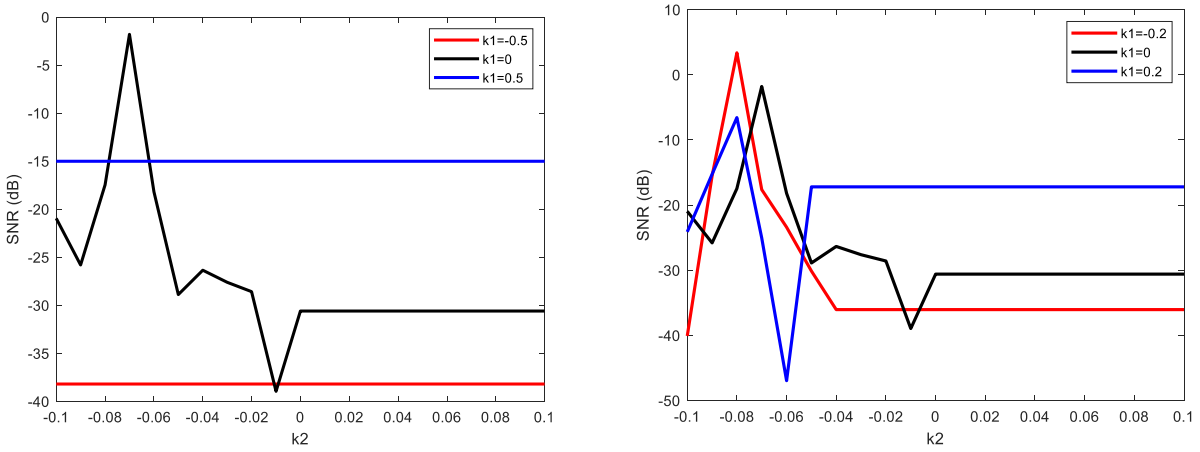


**Fig. 9.** Changes in SNR with k2 under different k1 effects of $\alpha$ noise.

objectives, and individual behavior. To select an appropriate parameter optimization algorithm, a comparison was conducted between the particle swarm optimization algorithm and the brainstorming algorithm during the experimental phase. Using the periodic signal $s(t) = A\sin(2\pi ft)$ with $\alpha$ noise, where$A = 0.01, f = 0.01$. When applying the above two algorithms to the system, while achieving the optimal correlation value, the running time of the algorithms should be minimized as much as possible. With the improvement of SNR, the evaluation of algorithms' strengths and weaknesses should be based on their performance on identical data under varying noise levels. Considering that the time required for a single execution of the same program may vary during runtime, this study documents the results and execution times of 50 independent runs, filters out data with significant fluctuations, and computes the average values to obtain experimental data, as presented in Tables 1 and 2.

Based on the aforementioned data, it is evident that while the convergence rate of the particle swarm optimization algorithm surpasses that of the brainstorming algorithm, the growth rate of the output SNR is lower in the particle swarm optimization. For signal processing, there is not much difference in convergence speed, so brainstorming algorithms are used in signal processing.

In order to achieve optimal parameter matching, the algorithm takes the output SNR as the objective optimization function. When the SNR reaches its maximum value, a set of corresponding system parameters is obtained, and adaptive detection of weak signals is achieved by adjusting the parameters. The algorithm process is shown in the figure:

## 4. System simulation

### *4.1. Single frequency periodic signal driven by α noise*

This section employs numerical simulation signal analysis to assess the efficacy of the proposed method. In a stable noise environment, the impact of a Gaussian bistable cascaded dual feedback system on periodic signals is analyzed using signal-to-noise ratio. The periodic signal $S(t) = A\sin(2\pi ft)$ under test is assumed to be mixed with noise, yielding a noise signal with an input signal-to-noise ratio of -31.88 dB. The time-domain waveform and spectrum of the simulated signal are shown in Fig. 10.

The noise parameter is set to: $\alpha = 1.2, \beta = 0, \sigma = 1, \mu = 0$. It is evident that the noise in the system output signal has been significantly reduced. Moreover, in the frequency spectrum, due to noise interference, the frequency amplitude of the target signal is small, resulting in low recognition. The optimal parameters obtained using BSO are$a = 2.13, b = 0.1, V = 0.1, R = 0.01, k_1 = -0.77, k_2 = 0.12$, respectively. The output results are shown in Fig. 11 (c) (d), where the system's output SNR=4.41dB. As a comparison, the cascaded SR method has also been used to process the simulated signals mentioned above, both employ the BSO algorithm for adaptive system parameter selection. The results obtained are depicted in Figs. 11(e) and (f). The output SNR is -4.39 dB. It is evident that the time-domain waveform still experiences substantial noise interference, and the signal's oscillation period is less distinct than that depicted in Fig. 11(c).

Obviously, compared with Fig. 11 (f) and Fig. 11 (d), Although the noise is significantly reduced compared to the original signal in the detection results shown in Fig. 11 (f), and the spectral peaks corresponding to the target signal frequency are relatively obvious in

**Table 1**
The impact of different algorithms on the output SNR.

| Noise intensity | SNRin | SNRout1(PSO) | SNRout(BSO) |
|---|---|---|---|
| D=0.1 | -29.81dB | 13.08dB | 13.93dB |
| D=0.3 | -31.83dB | 7.87dB | 8.18dB |
| D=0.5 | -32.55dB | 6.35dB | 7.23dB |
| D=1 | -33.35dB | 1.43dB | 1.69dB |

**Table 2**
Average time for different algorithms to achieve optimal results (50 independent runs).

| Noise background | Number of particles | Iterations | PSO | BSO |
|---|---|---|---|---|
| $\alpha$ noise | 30 | 100 | 7.51 | 8.11 |
| Gaussian noise | 30 | 100 | 7.32 | 8.06 |

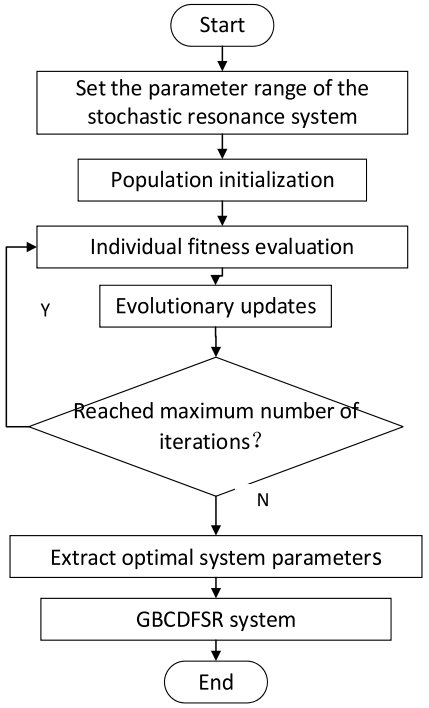


**Fig. 10.** Flow chart of adaptive SR based on BSO algorithm.

the spectrum, it is evident that the time-domain waveform obtained by the method proposed in this paper has more obvious periodicity, and the peaks corresponding to the target signal frequency in the frequency spectrum are more prominent. That is to say, the method proposed in this article has better detection performance for weak signals than simple cascading methods.

In practical engineering, most signals are high-frequency signals. With a single high-frequency signal as the research subject, the frequency of the input signal is considered. By mixing the signal with noise, a noise signal with an input SNR of -31.92 dB is achieved. Using the BSO optimization algorithm, the system optimization parameters $a = 8.02, b = 3.40, V = 3.72, R = 2.51, k_1 = -1.07, k_2 = 1.62$can be obtained. At this time, the output SNR=5.06dB. Compared to the input signal, the SNR has increased by 36.98dB. Fig. 12

### 4.2. Multi frequency periodic signals driven by α noise

When studying the adaptive multi steady state SR phenomenon driven by multiple low-frequency periodic signals, multiple low-frequency noisy input signals are shown in equation (11):

$$s(t) = A_1\sin(2\pi f_1 t) + A_2\sin(2\pi f_2 t) + A_3\sin(2\pi f_3 t) + D\xi_\alpha(t). \tag{11}$$

Among them, the amplitude of the periodic signal:$A_1 = A_2 = A_3 = 0.01$, The signal frequencies are$f_1 = 0.01Hz, f_2 = 0.03Hz, f_3 = 0.03Hz$, $\xi_\alpha(t)$ by $\alpha$ Stable noise, The strength is$D = 0.1$, The noise parameters are set to: $\alpha = 1.2, \beta = 0, \sigma = 1, \mu = 0$, Mixing the signal with noise results in a noise signal with an input SNR of -30.65dB. Using the BSO algorithm for optimization, the system optimization parameters $a = 2.14, b = 0.1, V = 0.1, R = 0.01, k_1 = -0.77, k_2 = 0.12$ can be obtained. At this point, the output SNR=-13.95dB. Fig. 13

Using a single high-frequency signal as the research object under the same noise background, i.e. the frequency of the input signal $f_1 = 100, f_2 = 300, f_3 = 500$, By mixing the signal with noise, a noise signal with an input SNR of -32.66dB is obtained. The system optimization parameters $a = 10.00, b = 0.10, V = 8.40, R = 5.43 k_1 = -2, k_2 = -0.43$ and the output SNR=-25.14dB Fig. 14.

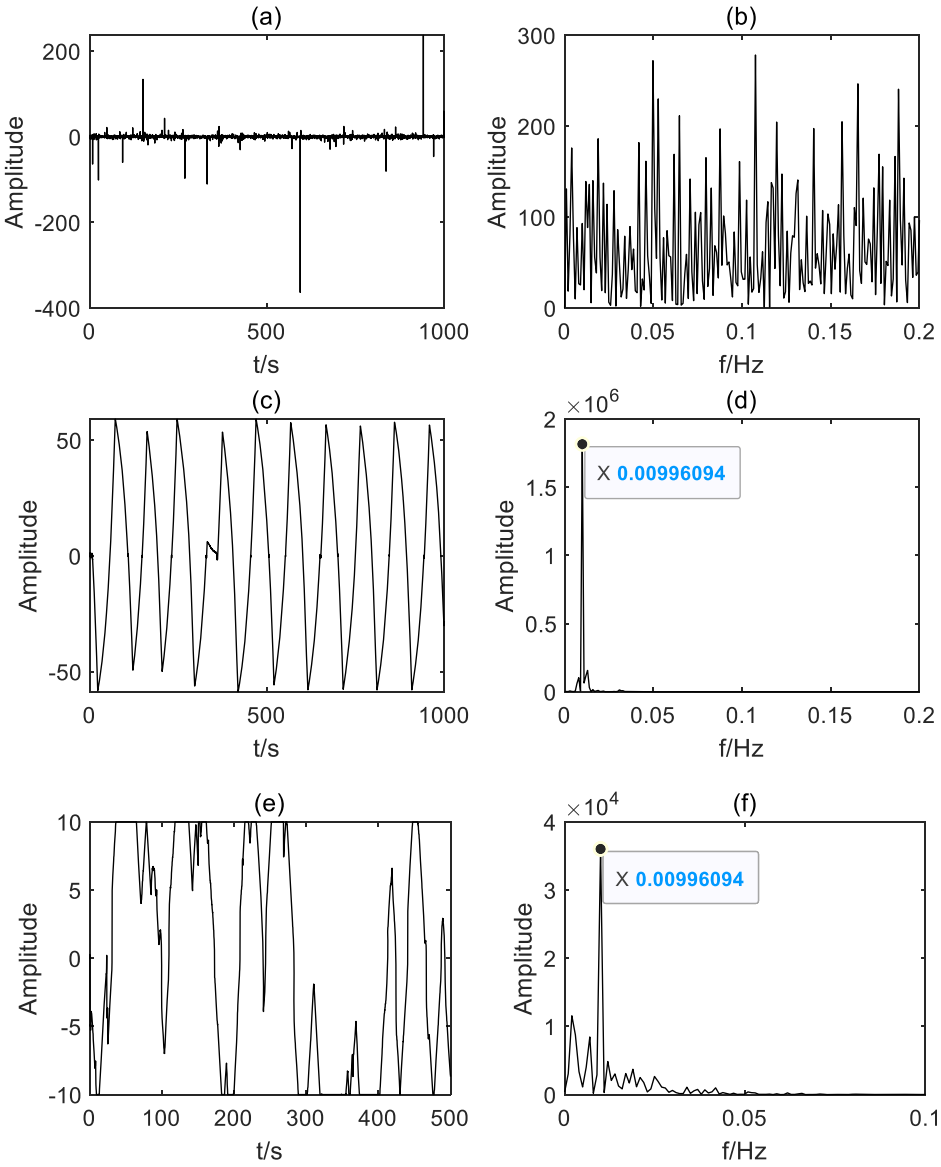


**Fig. 11.** Detection of a single high-frequency periodic signal under $\alpha$ noise in a Gaussian bistable cascaded dual feedback system.

## 5. Engineering applications

Bearings are ubiquitous in industrial settings and play a critical role in these environments. Bearings that develop faults require periodic maintenance, which, if not addressed, can lead to disastrous outcomes and significant economic losses. Therefore, monitoring and fault diagnosis of bearings during operation are of great significance. Usually, fault vibration data is obtained through an accelerometer installed on the bearing device. It should be noted that these data contain noise between the accelerometer and bearing contact surface, as well as noise in the industrial environment, and these signals exhibit multi-scale noise [25,26]. In this section, we will employ the adaptive GBCDFSR system introduced in this paper to analyze fault data, aiming to effectively pinpoint the fault characteristics of the bearings. The research object in this article is the deep groove ball bearing with the bearing model 6205-2RS JEM SKF. Its main structural parameters are shown in Table 3. Based on the different bearing types and speeds [27], the fault characteristic frequency can be theoretically calculated as follows:

$$f_I = \frac{r}{60} \times \frac{1}{2}\left(1 + d\frac{D}{\cos\alpha}\right), \tag{12}$$

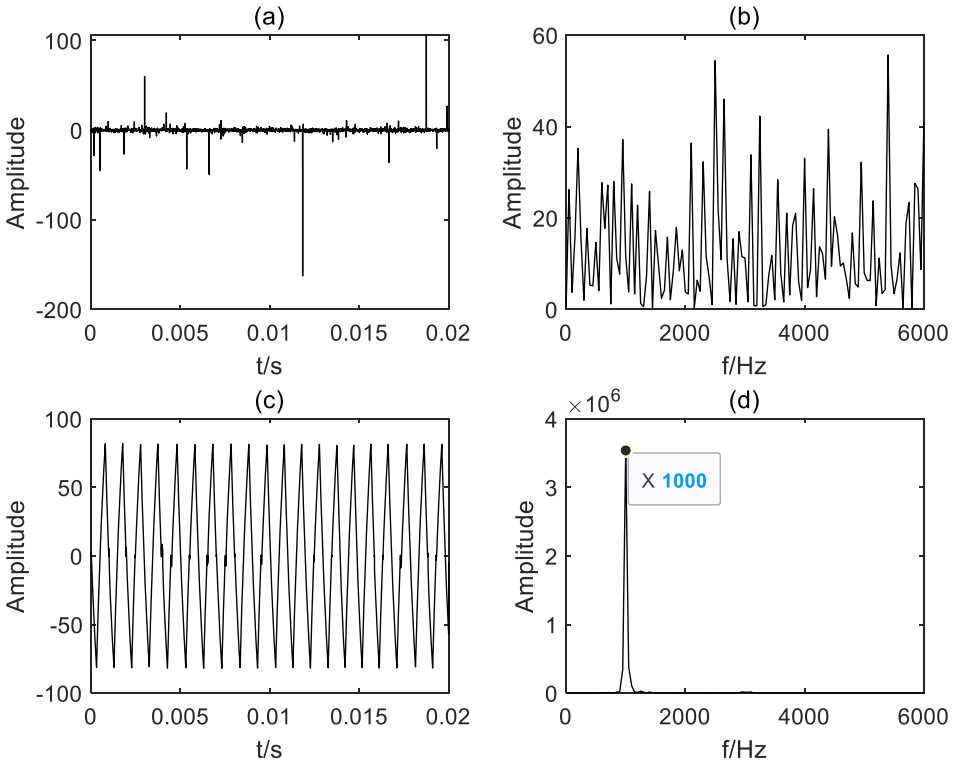


**Fig. 12.** Detection of a single high-frequency periodic signal under $\alpha$ noise in a Gaussian bistable cascaded dual feedback system.

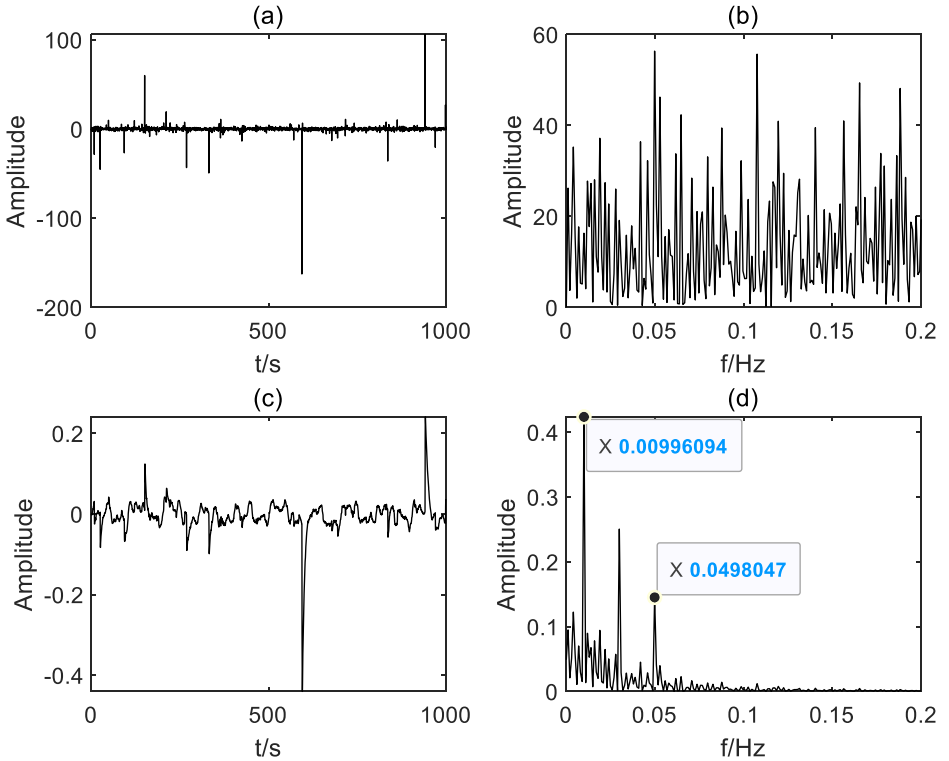


**Fig. 13.** Multiple low-frequency periodic signals detected under $\alpha$ noise in a Gaussian bistable cascaded dual feedback system.

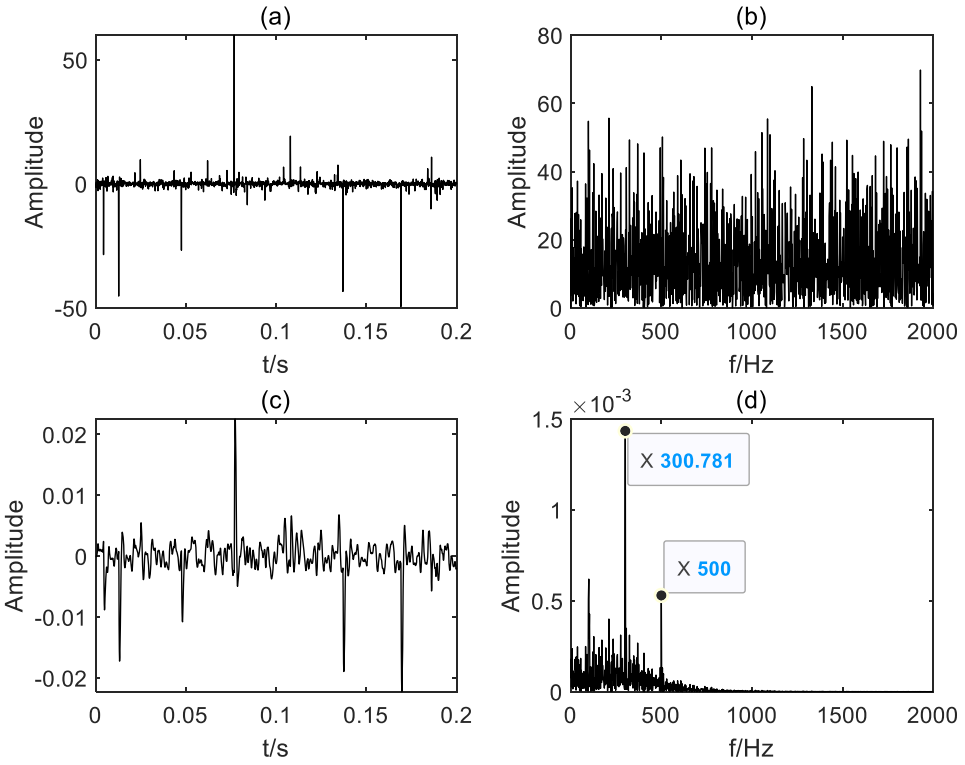


**Fig. 14.** Multiple high-frequency periodic signals detected under $\alpha$ noise in a Gaussian bistable cascaded dual feedback system.

**Table 3**
Parameters of rolling bearing.

| Internal diameter (feet) | External diameter (feet) | Thickness (feet) | Ball diameter (feet) | Middle diameter (feet) | Number of ball bearings |
|---|---|---|---|---|---|
| 0.9843 | 2.0472 | 0.5906 | 0.3126 | 1.537 | 9 |

$$f_O = \frac{r}{60} \times \frac{1}{2}\left(1 - d\frac{D}{\cos\alpha}\right). \tag{13}$$

In the formula, $f_O$ represents the frequency of outer ring faults; $f_I$ represents the frequency of inner ring faults; $r$ represents the rotational speed of the bearing and$r = 1772r/\min$; D represents the number of ball bearings $d, D$ Represent the ball diameter and bearing pitch diameter respectively; $\alpha$ indicates the contact angle of the rolling element $\alpha = 0$.

When the diameter of the fault is 0.007 inches and the depth of the fault is 0.011 inches, the fault frequencies of the inner and outer rings can be calculated to be 159.91 Hz and 105.86 Hz. Separately detect the fault signals of the inner and outer rings of the bearing [27].

### 5.1. *Bearing outer ring fault signal*

Firstly, process the bearing outer ring fault signal data from the official bearing data website of Case Western Reserve University. The fault signal is processed using the adaptive GBCDFSR weak signal detection method based on BSO proposed in this paper. Due to the downloaded signal not conforming to the adiabatic approximation theory, we resampled the signal with a sampling frequency of 12 kHz and 8000 sampling points. In time-domain Fig. 15 (a), due to the presence of noise, the time-domain characteristics of the signal cannot be clearly observed. In power spectrum 15 (b), the fault characteristic frequency component is covered by the noise component, and the frequency band is mainly concentrated between 2500 Hz–4000 Hz.

By optimizing the BSO parameters, the system output signals with system parameters of: can be obtained, as shown in Fig. 16.

### 5.2. *Bearing inner ring fault signal*

Fig. 17 depicts the fault signal of the bearing inner ring, which is also obtained from the official bearing data website of Case

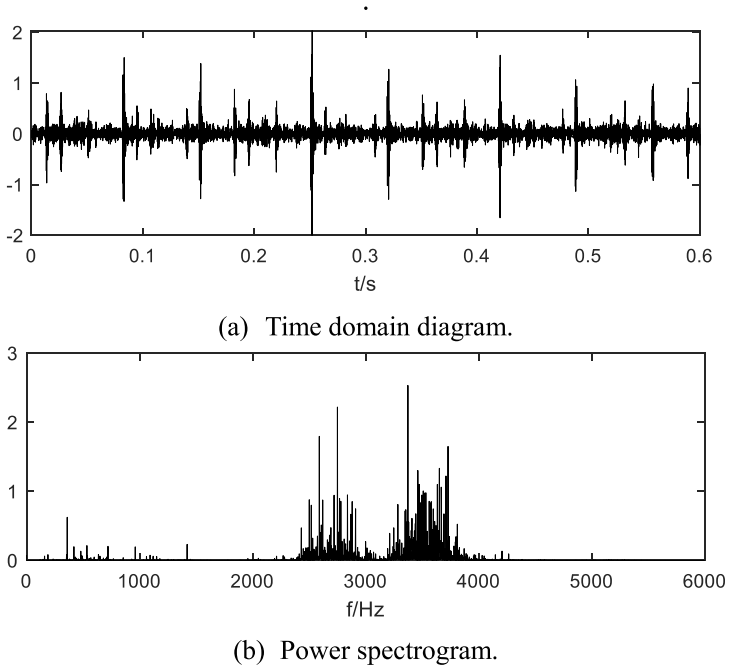


**Fig. 15.** Fault signal of outer ring bearing.

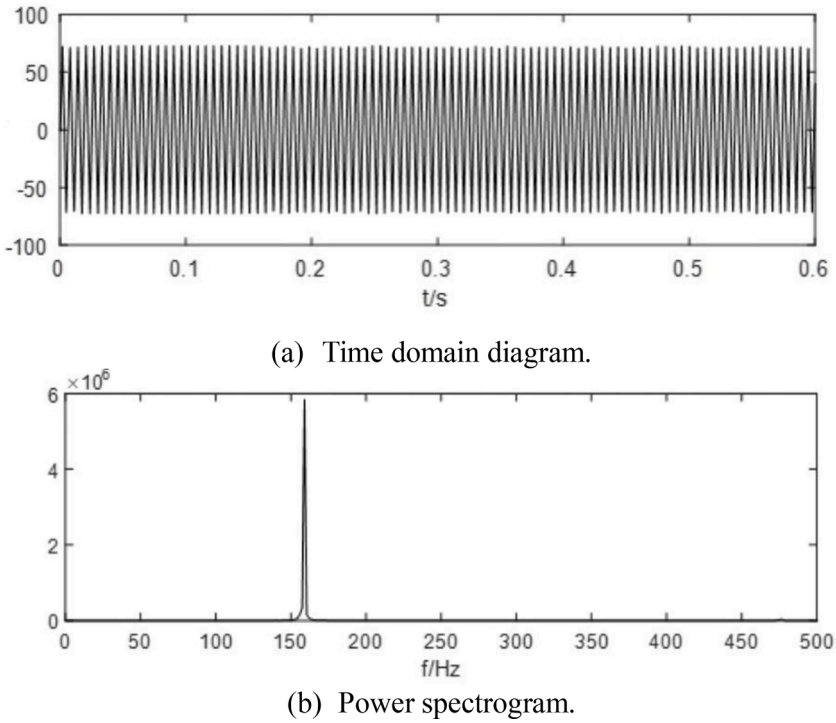


**Fig. 16.** Output of GBCDFSR system.

Western Reserve University. The inner ring fault signal is re-sampled with a sampling frequency of 1.2 kHz and 8,000 sampling points.

Using the same processing method as the outer ring fault signal, the system parameters $a = 12.13, b = 4.64, V = 5.47, R = 50.78$, $k_1 = 1.88, k_2 = 0.50$ can be obtained through BSO algorithm optimization, as shown in Fig. 18.

In this section, the re-sampled fault data will serve as input for the adaptive SR system. The frequency domain waveform of the output signal exhibits certain periodicity, as evident from both its time domain and power spectrum. Spike pulses are observed at

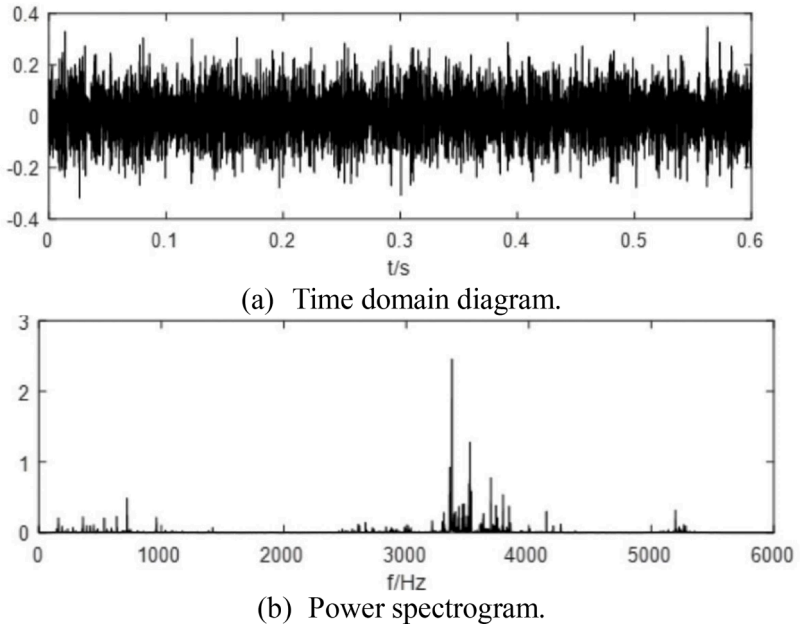


**Fig. 17.** Inner ring bearing fault signal.

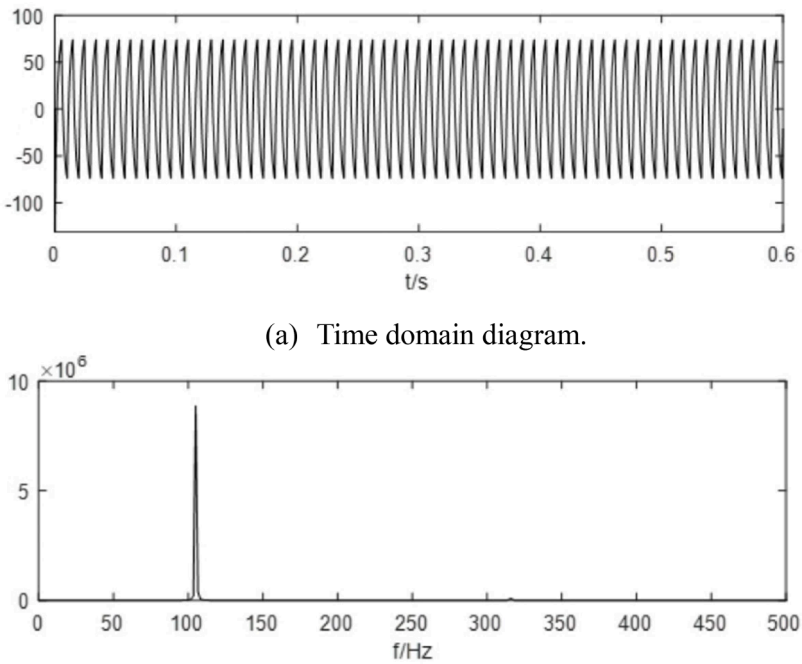


**Fig. 18.** Output of GBCDFSR system.

frequencies of 159.72Hz and 105.70Hz, which align with the theoretically calculated frequency of the bearing fault signal, maintaining an error of less than 0.2Hz. The adaptive parameter-induced GBCDFSR detection method introduced in this study can effectively detect faint fault signals, facilitating early fault diagnosis and minimizing losses.

## 6. Summary

In this paper, the GBCDFSR system is constructed, and the relationship between the system output signal-to-noise ratio and the noise intensity is studied. Compared with the Gaussian bistable cascade system without feedback link, the superiority of the feedback link is proved. The introduction of output feedback not only enhances the utilization of noise energy, but also improves the stability and robustness of the system. When the system is subject to external disturbances or parameter changes, the feedback mechanism can adjust the system in time to suppress fluctuations and instability, so as to maintain the stable operation of the system. Most importantly, output feedback enables the system to have a memory function, that is, the system can use the output information to optimize the current processing process. This memory function can help the system better understand and recognize the patterns and features of the input signal, so as to improve the extraction and recognition of the feature frequency. It can obviously enhance the signal-to-noise ratio of the output signal and the recognition degree of the characteristic frequency. The system is applied to the detection of multi frequency (high frequency, low frequency) weak periodic signals in $\alpha$ stable noise environment, and the simulation results verify the effectiveness of the system. Finally, the method is applied to bearing fault diagnosis, and the weak fault signal submerged in noise is effectively detected.

## Funding

Project supported by the National Natural Science Foundation of China (No. 62371388, 62127809), The key research and development projects in Shaanxi Province (No. 2022JBGS3-01), Qin Chuangyuan Innovation Platform (No. 23TSPT0002), Scientists + Engineers Team (No. 23KGDW0011,2024QCY-KXJ-014)

## CRediT authorship contribution statement

**Shangbin Jiao:** Writing – review & editing. **Tiantian Hou:** Writing – review & editing, Writing – original draft. **Tingyang Jiao:** Writing – review & editing. **Yi Wang:** Writing – review & editing. **Nianlong Song:** Writing – review & editing.

## Declaration of competing interest

The authors declare that they have no known competing financial interests or personal relationships that could have appeared to influence the work reported in this paper.

## References

[1] Z Shuai, S Peiming, Mechanical fault feature extraction under underdamped conditions based on unsaturated piecewise tri-stable stochastic resonance[J], Appl. Sci. 13 (2) (2023) 908, 908.
[2] Y Li, Q Zhu, Y Xu, et al., Enhanced fault diagnosis via stochastic resonance in a piecewise asymmetric bistable system.[J], Chaos. 34 (1) (2024).
[3] S B Jiao, D Sun, D Liu, et al., Research on the weak signal detection method based on adaptive vibrational resonance[C], in: The 35th Chinese Control Conference, Chengdu, China 7, 2016, 27-2016.7.29.
[4] Z Gang, H Xiaoxiao, X Jiaqi, et al., Adaptive detection of impact signals with two-dimensional piecewise tri-stable stochastic resonance and its application in bearing fault diagnosis[J], Appl. Acoust. (2023) 214.
[5] Y Mingyue, W Pengda, S Jingwen, et al., Self-adaptive stochastic resonance rub-impact fault identification grounded on a new signal evaluation index[J], J. Fail. Anal. Prev. 23 (5) (2023) 2118–2130.
[6] Gang Zhang, Yichen Shu, Tianqi Zhang, Piecewise unsaturated multi-stable stochastic resonance under trichotomous noise and its application in bearing fault diagnosis[J], Results. Phys. 30 (2021) 104907.
[7] H.S. Wio, S. Bouzat, Stochastic resonance: the role of potential asymmetry and non gaussian noises[J], Braz. J. Phys." 29 (1) (1999) 136–143.
[8] G Zhang, DY Hu, TQ. Zhang, Bearing fault diagnosis based on unsaturated piecewise non-linear bistable stochastic resonance under trichotomous noise[J], Fluct. Noise. Lett. 19 (3) (2020) 2050024.
[9] G Zhang, YL Yang, TQ. Zhang, The characteristic analysis of stochastic resonance and bearing fault diagnosis based on nwsg model driven by trichotomous noise [J], Chin. J. Phys. 60 (2019) 107–121.
[10] SB Jiao, XX Qiao, S Lei, et al., A novel parameter-induced adaptive stochastic resonance system based on composite multi-stable potential model[J], Chin. J. Phys. 59 (2019) 138–152.
[11] Z. Li, B. Shi, A piecewise nonlinear stochastic resonance method and its application to incipient fault diagnosis of machinery, Chin, J. Phys. 59 (2019) 126–137.
[12] W. Cheng, X. Xu, Y. Ding, K. Sun, Q. Li, L. Dong, An adaptive smooth unsaturated bistable stochastic resonance system and its application in rolling bearing fault diagnosis, Chin, J. Phys. 65 (2020) 629–641.
[13] P.M. Shi, Q. Li, D.Y. Han, Stochastic resonance in a new asymmetric bistable system driven by unrelated multiplicative and additive noise[J], Chin. J. Phys. 54 (4) (2016) 526–532.
[14] H. Li, R. Bao, B. Xu, et al., Intrawell stochastic resonance of bistable system, J. Sound Vib. 272 (1–2) (2004) 155–167.
[15] L Jimeng, C Xing, P Junling, et al., A new adaptive parallel resonance system based on cascaded feedback model of vibrational resonance and stochastic resonance and its application in fault detection of rolling bearings[J], Chaos, Solitons and Fractals: the interdisciplinary journal of Nonlinear Science, and Nonequilibrium and Complex Phenomena (2022) 164.
[16] W Cui, S Jiao, Q Zhang, et al., Dual-channel two-dimensional stochastic resonance and its application in bearing fault detection under alpha-stable noise[J], . Chin. J. Phys. 88922 (2024) 937.
[17] R Zhang, L Meng, L Yu, et al., Collective dynamics of fluctuating–damping coupled oscillators in network structures: Stability, synchronism, and resonant behaviors[J], Phys. A: Stat. Mech. Appl. (2024) 638129628. -.
[18] S Jian, W Haiyan, S Xiaohong, et al., Mutual information-assisted feed-forward cascaded stochastic resonance for large parameter[J], Nonlinear. Dyn. 111 (20) (2023) 19225–19247.
[19] Z Gang, L Xiaoman, Z Tianqi, Two-dimensional tri-stable stochastic resonance system and its application in bearing fault detection[J], Phys. A: Stat. Mech. Appl. (2022) 592.
[20] L Jian, G Jiaqi, H Bing, et al., Controlled symmetry with woods-saxon stochastic resonance enabled weak fault detection.[J], Sensors. (Basel) 23 (11) (2023).

[21] L Xu, G Zhang, L Bi, et al., Stochastic resonance in hindmarsh-rose neural model driven by multiplicative and additive gaussian noise[J], Phys. Scr. 99 (1) (2024).
[22] Z Gang, L Xiaoman, Z Tianqi, Two-dimensional tri-stable stochastic resonance system and its application in bearing fault detection[J], Phys. A: Stat. Mech. Appl. (2022) 592.
[23] L Wu, Z He, Y Chen, et al., Brainstorming-based ant colony optimization for vehicle routing with soft time windows.[J], IEEe Access. 719643 (2019) 19652.
[24] N Z Run, S X Hua, M Yan, et al., Quantum particle swarm optimization algorithm with the truncated mean stabilization strategy[J], Quantum. Inf. Process. 21 (2) (2022).
[25] P Xia, M Lei, H Xu, et al., Fault diagnosis of rolling bearing based on the three-dimensional coupled periodic potential-induced stochastic resonance[J], Meas. Sci. Technol. 35 (4) (2024).
[26] L Jimeng, P Junling, Z Shi, et al., Weak fault feature extraction of rolling bearing based on multi-system coupled cascaded stochastic resonance system[J], Meas. Sci. Technol. 35 (3) (2024).
[27] H Liang, J Wu, W Zhang, et al., Guided wave localization of small defects based on stochastic resonance characteristics of Duffing systems[J], Int. J. Press. Vessels Pip. (2024) 209105215.